IACC Appendage Studies

E. N. Tinoco, The Boeing Company, Seattle, Washington, USA
A. E. Gentry, The Boeing Company, Seattle, Washington, USA
P. Bogataj, The Boeing Company, Seattle, Washington, USA
E. G. Sevigny, The Boeing Company, Seattle, Washington, USA
B. Chance, Chance & Company, Inc., Essex, Connecticut, USA

ABSTRACT

Experimental and computational studies of several representative IACC appendage geometries were carried out to establish baseline data and verify computational models and methods.

Wind tunnel tests of an unheeled, unswept, constant section, rectangular planform keel mounted on a ground plane included force and moment measurements, and wake surveys at various angles of attack. Test configurations (all at constant draft) included the addition of ballast bulbs and winglets.

Correlations of computational results with experimental wind tunnel data were made. A502/PAN AIR potential flow induced drag predictions proved to be in good agreement with the wind tunnel data. Comparisons are also presented between A598 (A502 + boundary layer), wind tunnel results and empirical predictions. Again good agreement was shown for cases within the limitations of the boundary layer method.

NOMENCLATURE

A1	-	Keel-bulb fairing
B1	-	Round bulb
B2	-	Beavertail bulb
b	-	wing or keel span
C_D	-	Drag (total) coefficient
C_d	-	Section drag coefficient
C_{DI}	-	Induced drag coefficient
C_{Do}	-	Zero-lift drag coefficient
C_{DP}	-	Profile drag coefficient
C_L	-	Lift coefficient
C_l	-	Section lift coefficient
C_{M25c}	-	Pitching moment about 25% chord line of the keel
dC_{DI}	-	Wind tunnel wall correction to induced drag
e	-	induced drag efficiency factor
h	-	vertical distance between wings
P	-	Pressure
S1	-	Keel
s	-	distance
U	-	Total velocity
u	-	Perturbation velocity in x-direction
v	-	Perturbation velocity in y-direction
w	-	Perturbation velocity in z-direction
W1.x	-	Short winglet
W2.x	-	Long winglet
x,y,z	-	Cartesian coordinates
α	-	angle of attack (leeway)
ρ	-	density
ξ	-	vorticity
ψ	-	Streamfunction

INTRODUCTION

Sailboats operate at the air/water interface, a free surface, permitting the formation of waves due to pressure disturbances - including lift - with consequential loss of energy downstream. The free surface is of particular importance in the IACC (International America's Cup Class) where performance and heel are high due to generous sail area, relatively low displacement and stability, and the high speeds developed. Ideally, full consideration should be given to this air/water interface in the development of the wetted portion of an IACC yacht. Free surface computational modeling codes are beginning to emerge from the developmental stage. However, they are costly to panel and run and may still be lacking in the reliability and accuracy required for modelling lifting conditions. Cost effective, reliable, and timely computational modelling decisions would have to accept some simplification.

Fortunately, most design interest was directed toward the study of representative ballast packages (bulbs) with and without winglets. It was reasoned that with the increased draft of the IACC class that the combined flow fields from the hull and bulb would allow the simplification of reflection plane models of keel/ballast packages alone. Reflection plane models are strictly

valid only at zero Froude number (zero speed) or at infinite Froude number when a plane of anti-symmetry is used. This approach is further reinforced by Reynold's number and blockage of large hull models, and cost considerations in available wind tunnels.

Attention was therefore directed at the development of CFD (Computational Fluid Dynamics) lift and induced, as well as viscous, drag methodologies and prediction techniques. The computational effort was combined with wind tunnel validation of the effects of tip tank like bulbs on a typical IACC keel and the effects of winglets on the keel/bulb combinations. Global optimization was not undertaken due to the free surface and other modelling issues. However, wind tunnel tests confirmed CFD predictions and formed a useful basis for the development of Stars & Stripes final keel and that on the successful defender America[3].

The results of a joint CFD (Computational Fluid Dynamics) and wind tunnel based study on generic appendages suitable for the new class of IACC yachts are presented. This work was sponsored by The Boeing Company in partnership with PACT (Partnership for America's Cup Technology). Computing resources necessary to support this work were made available through PACT by Cray Research and IBM. The study focused on establishing a parametric experimental data base of keel, ballast bulbs, and winglet configurations, and the validation of CFD tools for their design and analysis. A wind tunnel test was conducted of configurations consisting of combinations of a single keel configuration, two bulb configurations, and two winglet configurations, each at two longitudinal positions on each bulb. Both force and wake survey data were obtained. The wake survey data was used in a Boeing-developed code that provided a mapping of spanwise lift, profile drag, and induced drag. The wake and force data were available to both PACT and the American syndicates, and as a validation data base for Computational Fluid Dynamics work.

GEOMETRY

A total of thirteen configurations were wind tunnel tested. These configurations were made up from the following basic parts illustrated in Figure 1; one keel, two bulbs, one fairing, and two sets of winglets. PACT supplied Boeing with the baseline geometry for keel S1, and bulb B1. Boeing then designed the additional parts that were then manufactured by PACT and supplied back to Boeing for wind tunnel testing.

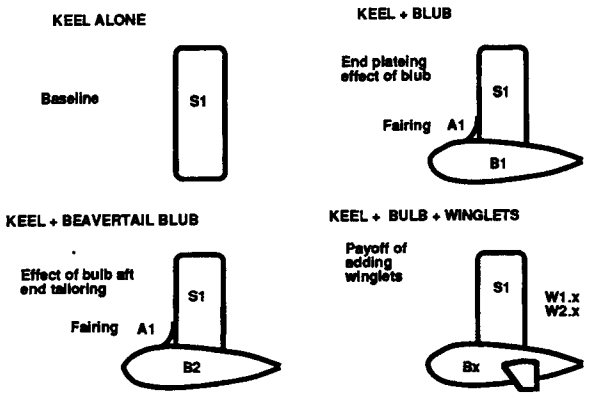

Figure 1. Wind Tunnel Test Configuration

The keel S1, has a 40.5 inch maximum span and a 16.75 inch chord with a NACA 63A009 section airfoil, Figure 2. The tip is finished off with circular arcs such that the diameter matches the keel thickness along the tip chord. The bulb B1, is axisymmetric with an airfoil section of a NACA 64A015 scaled up to 16.7% maximum thickness, a length of 56.293 inches, and a maximum diameter of 9.401 inches, Figure 3. Bulb B2, from the nose to 22.5 inches aft is identical to bulb B1, and has a total length of 48.109 inches. The aft section is two dimensional in character with a constant width equal to the maximum diameter, Figure 4. Both bulbs had the same volume. Two sets of winglets were made, both having root chords of 6.5 inches, tip chords of 2.0 inches, Figure 5. Winglet airfoils are symmetric NACA 64A010 sections . No twist was incorporated into either set of winglets. When attached to the bulb B1 in the forward position, winglets W1, have a planview semispan of 17.4 inches, while winglets W2, have a semispan of 25.0 inches. Both pairs of winglets have anhedral such that the tip reference chord coincides with the maximum keel span of 40.5 inches. The forward winglet positions, Wx.1, were positioned such that the trailing edges of the winglets were aligned with the trailing edge of the keel. The aft winglet positions were constrained by structural mounting requirements but were as far aft as practical. A wing-body strake fairing A1, was designed to reduce the classic vortex which forms at that intersection and thereby reduce the associated drag, Figure 6.

Boundary layer trips were used on the model to stabilize the position of turbulent transition. The round epoxy trip disks had a height of 0.01 inches. The trip disks were placed on both sides of the keel and winglets 1.0 inch aft of the leading edge in plan view, and the bulbs had a ring of disks 2.0 inches aft of the nose in side view. Sublimation type flow visualization was used to

verify that the trips were effective. There were no corrections to the force data for the drag of the trips.

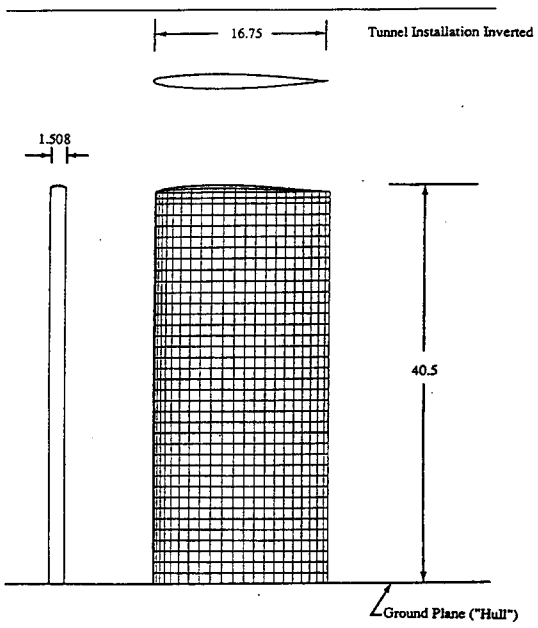

Figure 2. Configuration S1 - Keel Alone

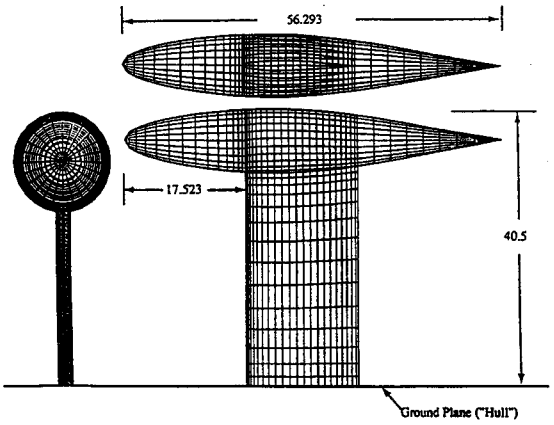

Figure 3. Configuration S1B1 - Keel + Round Bulb

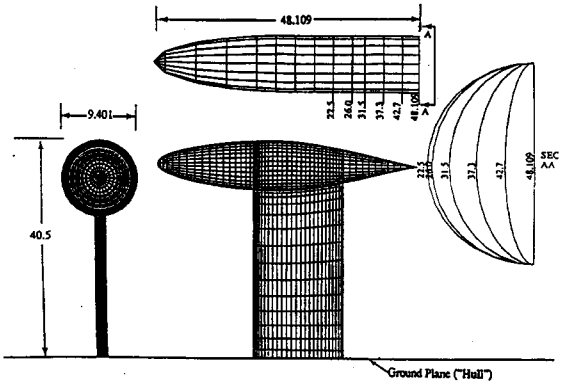

Figure 4. Configuration S1B2 - Keel + Beavertail Bulb

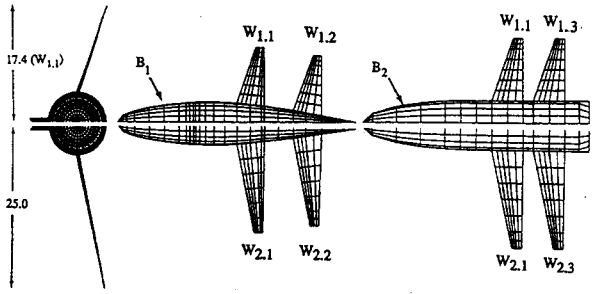

Figure 5. Positioning of Winglets on Bulbs B1 and B2

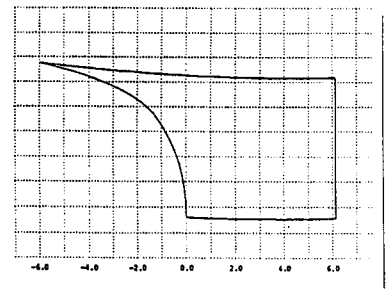

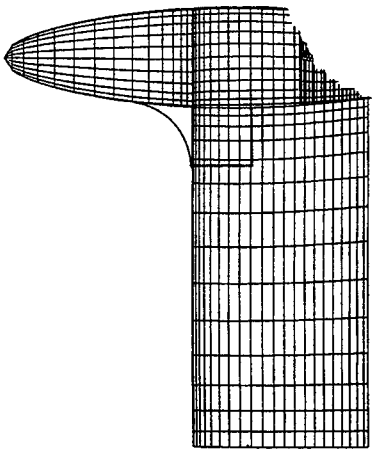

Figure 6. Strake Fairing Configuration on Either Bulb

WIND TUNNEL TEST DESCRIPTION

The wind tunnel facility used was the University of Washington Aerodynamics Laboratory (UWAL) low speed wind tunnel. This tunnel is a continuous, double return, atmospheric type tunnel. The test section and model installation is illustrated in Figure 7. The test section is rectangular with triangular fillets in all four corners. The width is 12 feet, the height is 8 feet, and the fillets are 1.5 feet high and wide

providing a cross sectional airflow area of 91.5 square feet. The six component force balance used is mounted below the tunnel floor. An eight foot square ground plane was installed which is centered on the balance with the top of the ground plane 6.345 inches above the tunnel floor. A turntable three feet in diameter is attached at it's center to the balance, and is centered on the ground plane. This turntable is the structure to which the inverted model is attached. A force drag tare for the turntable which included the effect of temperature on the skin friction was subtracted from the measured balance drag. The nominal test conditions were a dynamic pressure of 65 pounds per square foot, 0.21 Mach number, and a Reynolds number per foot of 1.35 million.

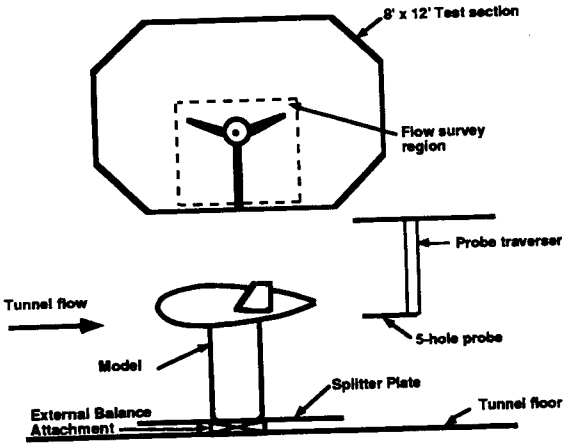

Figure 7. Wind Tunnel Installation

The wake survey analysis procedure required three component velocity data and axial total head data in a plane perpendicular to the reference free stream flow and immediately behind the model. To obtain this flow data a traversing five-hole pitot static cone head probe is used. The wake survey mechanism and an installed model are shown in Figure 8. The vertical struts penetrating the ceiling are attached to a motor drive such that they can be moved to any desired vertical position. The cross bar attached at the bottom of the vertical struts supports a motor driven radial arm to which is attached a five-hole pitot static probe. The arm is programmed to sweep out an arc, stop while the vertical mechanism increments a step, and then sweep back, etc, etc, all the while probe data is being taken on the fly while the radial arm is sweeping. The coverage area need only be large enough to capture the velocity deficit and the non-zero vorticity field. It is not necessary to sweep a very large region that has far field total pressure and zero vorticity even though the flow is deflected.

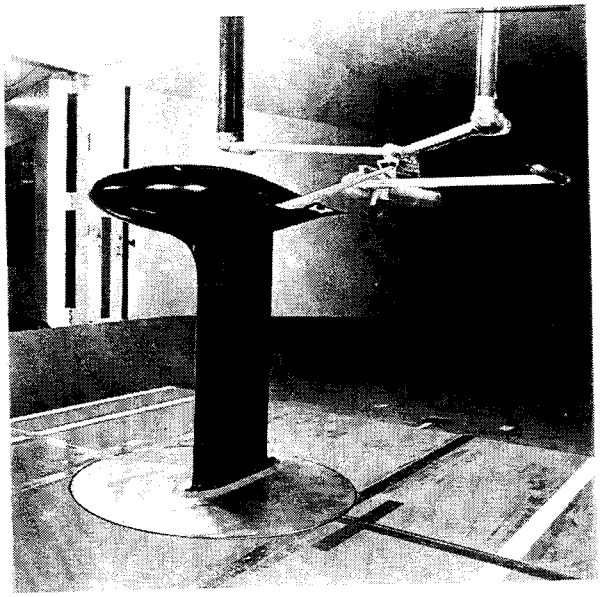

Figure 8. Wind Tunnel Model Installation with Wake Survey Rig

TEST RESULTS

Thirteen configuration combinations were tested measuring force data and eight of these were selected for wake survey analysis. Representative results from the test follow.

Force Data Results

Multiple runs of most configurations were done to check repeatability. The one sigma drag repeatability is 1 1/4 counts. One drag count is 0.0001 drag coefficient or 0.00047 square feet of drag area. The angle of attack (leeway angle) range is -2 degrees to 12 degrees if balance limits permitted.

Both longitudinal and lateral force/moment data were obtained for the thirteen configurations. The trends observed were as expected. That is, zero lift drag varies with wetted area including the beavertail bulb B2 drag being greater than the axisymmetric B1 by approximately the 3% wetted area increment. Induced drag is increased by the addition of either bulb to the keel. The beavertail bulb B2, reduces induced drag relative to the axisymmetric bulb B1. Winglets further reduce induced drag as expected. The keel lift curve slope for keel alone is increased about 5% with either bulb added, and increased nearly 9% to 12% with the addition of the winglets. The lift center of pressure locations, both longitudinal and lateral were also obtained in the linear region.

Summary comparison plots of the force data for several of the configurations tested are presented to illustrate typical results and

comparative performance. Data presented includes longitudinal lift vs. angle of attack (leeway) and pitching moment, the classic drag polar, and a profile drag polar where an ideal reference span induced drag has been subtracted from the total drag level. The profile drag polar format allows increased scale sensitivity for easier comparison of induced and profile drag differences between various configurations. Figures 9 thorough 11 illustrate the effects of adding the axisymmetric bulb B1 to the keel, the strake fairing A1, and then the smaller winglet W1 in the forward position to the bulb. The addition of a bulb to the keel is detrimental to performance from both a wetted area/profile drag standpoint and induced drag standpoint. Obviously, the bulb must increase sailing efficiency by reducing the boat's heeling angle if it is to be a benefit. The addition of the smaller winglet W1, to the bulb is seen to be beneficial above lift coefficients of 0.25 or angles of attack of 3.5 degrees relative to the bulb without the winglet. The addition of the strake fairing indicates up to an eight count benefit or 3% drag reduction for bulb B1. Figure 12 shows the profile drag polar effects of the two bulbs with and without winglets. Without winglets the beavertail bulb, in comparison to the axisymmetric bulb, reduces induced drag significantly, at the cost of slightly increased zero lift drag corresponding to its higher wetted area. Thus, the beavertail bulb is better than the axisymmetric bulb above lift coefficients of 0.17 or angles of attack of 3 degrees. However, with the addition of the winglets, the axisymmetric bulb has the best drag performance.

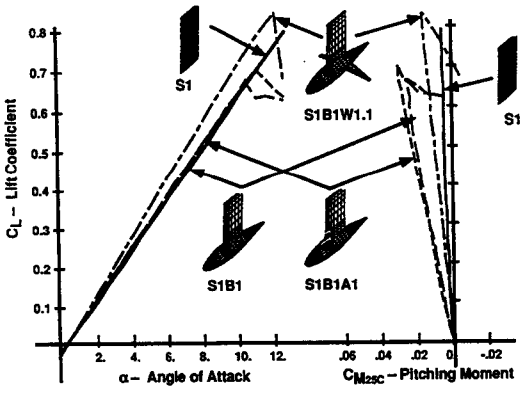

Figure 9. Comparison of Lift and Pitching Moment Characteristics: S1, S1B1, S1B1A1, S1B1W1.1

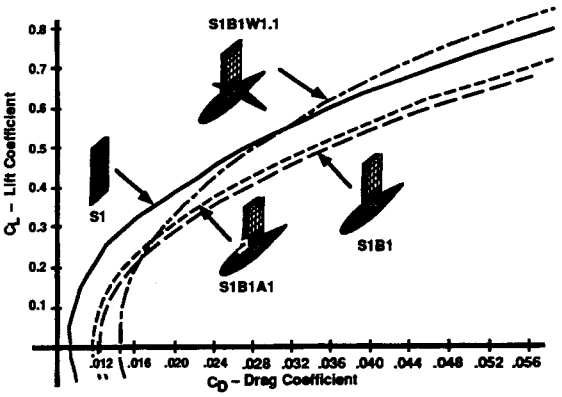

Figure 10. Comparison of Drag Polar Characteristics: S1, S1B1, S1B1A1, S1B1W1.1

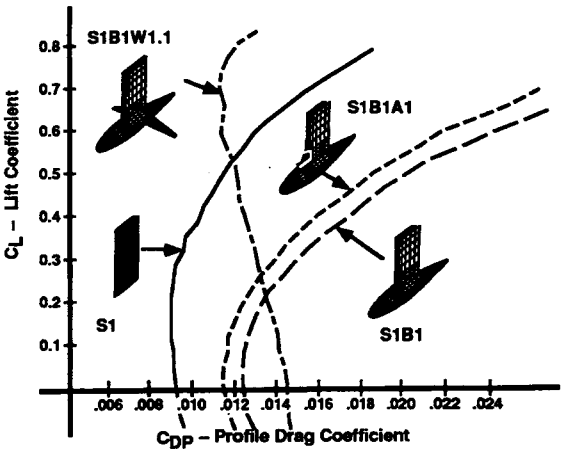

Figure 11. Comparison of Profile Drag Charastics: S1, S1B1, S1B1W1.1, S1B2W1.1

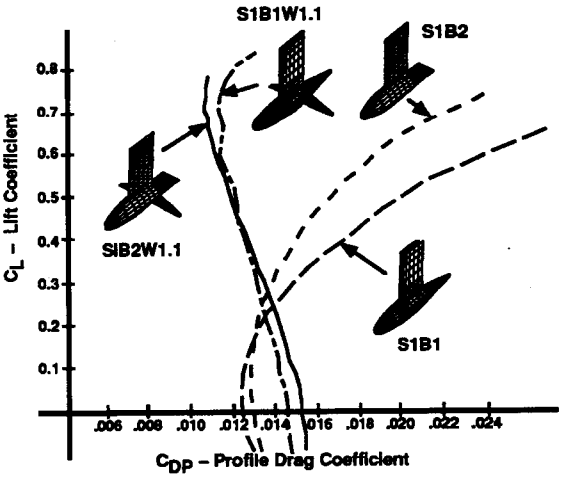

Figure 12. Comparison of Profile Drag Characteristics: S1B1, S1B2, S1B1W1.1, S1B2W1.1

Wake Survey Integrations

A wake survey is the collection of three component velocity, and pitot static data in a plane immediately behind the model and perpendicular to the axial centerline of the tunnel. These data are then processed by the wake survey analysis code to produce wake mappings of vorticity, profile drag, and induced drag. These mappings can then be integrated to determine the total lift, profile drag, and induced drag, or partially integrated to obtain spanwise effects. The wake survey analysis code is grounded on momentum theory. The basic momentum equation is rearranged to be a function of total head deficit, axial velocity deficit, and cross flow velocity terms. The first two terms are essentially profile drag and the third term is induced drag. The profile drag terms are manipulated relative to freestream to indicate zero as soon as the energy level reaches that of freestream. The induced drag crossflow terms are then reworked into functions of vorticity and potential stream function. These are functions of parameters that are non-zero only in the immediate wake region of the flow. The outline of the equation transformation is indicated in Figure 13. The physical/mathematical background and details are described in the references 1 to 5.

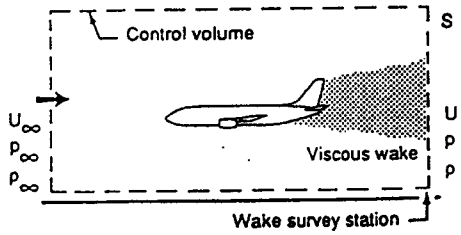

DRAG

$$\text{Drag} = \rho\iint(U^2_\infty - U^2)ds + (P_e - P)ds \quad \text{(momentum)}$$

$$= \iint_{wake}(P_{t_\infty} - P_t)ds + \tfrac{\rho}{2}\iint_{Tunnel}(U^2_\infty - U^2)ds \quad \text{(profile drag)}$$

$$+ \tfrac{\rho}{2}\iint_{Tunnel}(v^2 + w^2)ds \quad \text{(induced drag)}$$

$$U'^2 \equiv U^2 + \tfrac{2}{\rho}(P_{t_\infty} - P_t) \qquad U_b \equiv \tfrac{1}{ST}(U^* - U)ds \quad \text{(blockage)}$$

$$U' \equiv U^* - U_\infty \qquad U_e \equiv U_\infty + U_b$$

$$\text{Drag profile} = \iint_{wake}[P_{t_\infty} - P_t + \tfrac{\rho}{2}(U^* - U)(U^* + U - 2U_e)]ds$$

$$\text{Drag induced} = \tfrac{\rho}{2}\iint_{wake}(\psi\xi)ds; \qquad \psi = \textit{streamfunction}, \quad \xi = \textit{vorticity}$$

where $\xi = \frac{\partial w}{\partial y} - \frac{\partial v}{\partial z}$

ψ solved for by $-\xi = \frac{\partial^2\psi}{\partial y^2} + \frac{\partial^2\psi}{\partial z^2}$ $\psi = 0$ at walls (boundary condition)

LIFT

$$c(y) \cdot c_\ell(y) = -2\iint_{wake}\xi ds$$

$$C_L = \tfrac{1}{ST}\int c(y) \cdot c\ell(y)dy$$

Figure 13. Outline of Wake Survey Theoretical Basis

The processed data from the wake survey analysis code can be provided in a variety of formats. One format provides contour maps of profile drag, induced drag, and the angle the free air is deflected by the presence of the configuration. Keep in mind that these data are computed from data measured in a plane downstream of the model; thus, these distribution values are in this plane also. The conservation of momentum does imply that the integrated values of lift and drag will not change with downstream movement, only that the distribution can change with the deflection of the streamlines. Profile drag contours for a winglet configuration, S1B1W1.1, are shown in Figure 14. Another format provides spanwise integrations indicating the section lift of the lifting surface, and both the induced drag and profile drag spanwise distributions. The integrated keel data for the keel alone, S1, is shown in Figure 15. For contrast, Figure 16 shows integrated keel data and Figure 17 provides integrated winglet data for a configuration with bulb and winglet, S1B1W1.1.

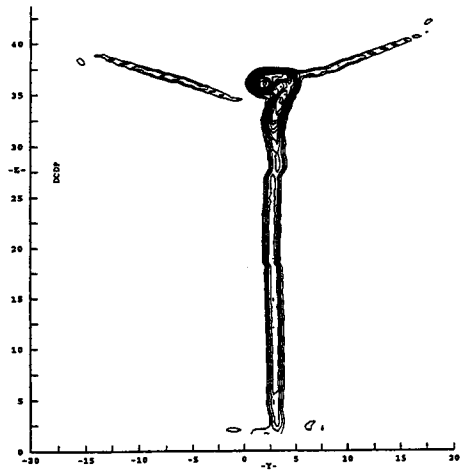

Figure 14. Profile Drag Isobars in Wake S1B1W1.1

Looking first at the distributions from the keel alone in Figure 15, note that the spanwise section lift distribution is relatively constant. This is because the keel is not twisted since it must operate symmetrically (sail on both tacks). Also note that the tip vortex has moved inboard from the physical 40.5 span to nearly 39 inches with the downwind movement to the wake survey plane. The induced drag is seen to be concentrated in the tip vortex and the profile drag is distributed uniformly along the span. For most cases there is an increase in the profile drag at the tip due to the vortex itself. This is probably due because the vortex sweeps the flow just inboard of the tip to capture some of the keel profile drag loss. At the "hull" end of the keel

there is a slight drop off due to not measuring the first 1.2 inches of keel span to prevent possible damage to the probe by contact with the ground plane.

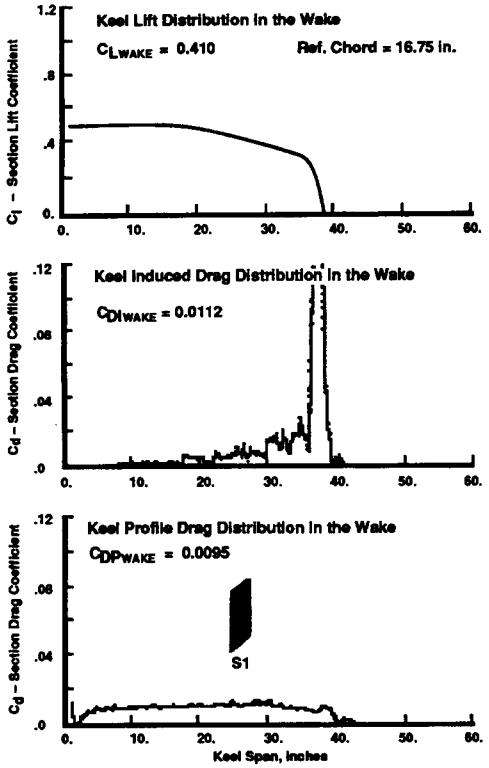

Figure 15. Keel Span Wake Summary: S1

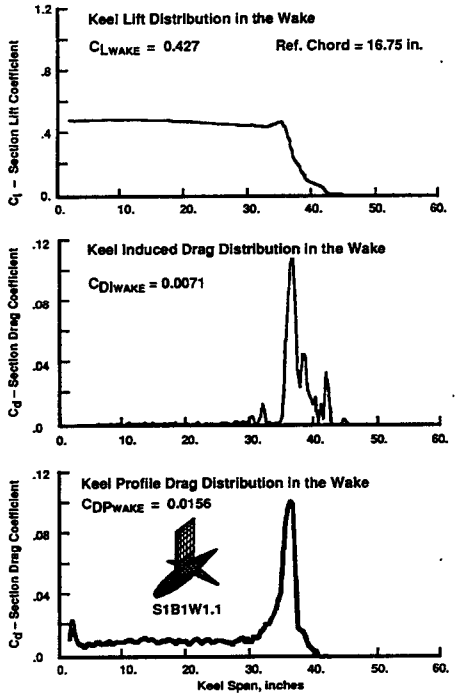

Figure 16: Keel Span Wake Summary: S1B1W1.1

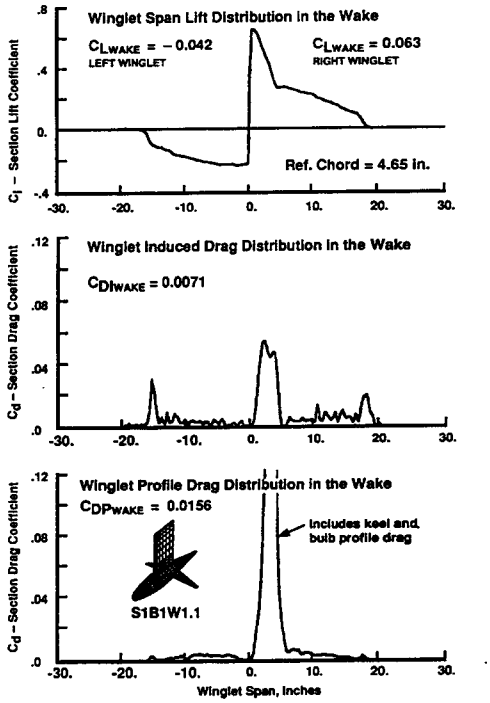

Figure 17. Winglet Span Wake Summary: S1B1W1.1

Figure 16 shows that the addition of the bulb and winglets returns the keel span loading nearly to the geometric span. Thus, the span efficiency is significantly improved, and the induced drag reduced. The keel span load is nearly constant along the keel span with significantly less loading across the bulb. Figure 17 illustrates the contribution from the winglets and bulb in the winglet spanwise direction. The upper figure shows the span loading of the winglet and bulb referenced to the winglet mean geometric chord. The center plot shows the induced drag due to the winglets except between the winglet roots where the keel and bulb effects are included. Finally the lower plot shows the profile drag due to the winglets including the contribution due to the keel and bulb.

The integrated results for both profile drag and the sum of profile plus induced drag have been compared to the force data polars. Comparisons for three of the configurations are shown in Figures 18 thorough 20. The wake survey analysis technique did accomplish the fundamental goals of determining lift, induced drag, and profile drag with reasonable accuracy. The one sigma variance for lift was 8.5 % and for drag was 7.8%, and the mean when compared to the force data results was within 2.0 %. The significance of this technique is the diagnostic capability it provides by being able to generate wake maps and

spanwise distributions of lift, induced drag, and profile drag. Thus, it can pinpoint the location of significant flow characteristics both good and bad.

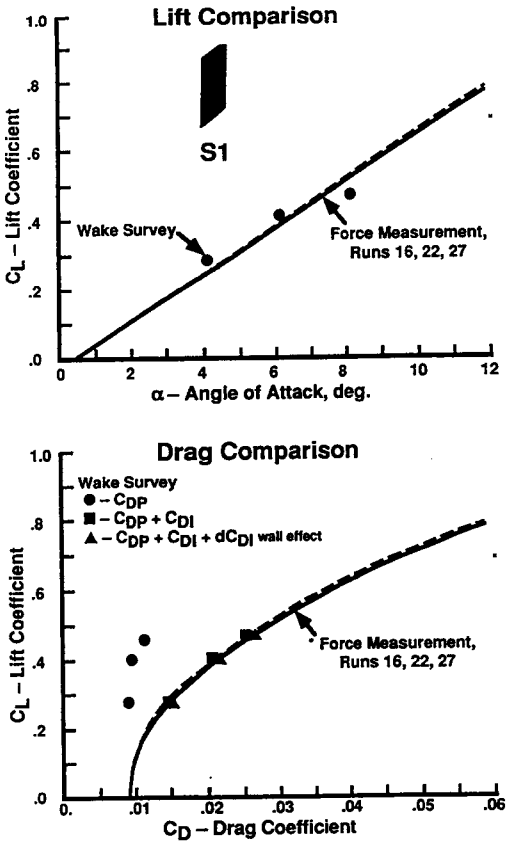

Figure 18. Wake Summary - Force Comparison: S1

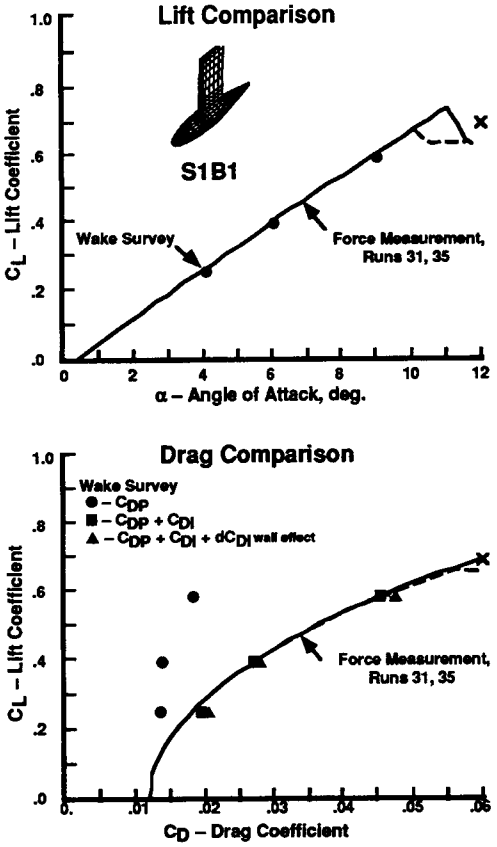

Figure 19. Wake Summary - Force Comparison: S1B1

COMPUTATIONAL STUDIES

Computational Fluid Dynamics (CFD) studies were conducted as a complementary and concurrent approach to the IACC appendage studies along with the wind tunnel testing. These studies focused on the hydrodynamics of the keel and associated appendages. Analyses included modeling of the hull and rudder in some instances. The free surface was for most of the studies treated as a solid reflection plane simulating a Froude number of zero. Capability also existed for using an anti-reflection plane simulating infinite Froude number.

The objective of the CFD studies was not just to demonstrate an ability to reasonably match experimental data after-the-fact. That is necessary to establish creditability, however. The objective was to develop a process by which key hydrodynamic performance characteristics of the appendages could be quickly and reliability calculated. These ingredients are necessary for effective use of CFD in developing new designs for which experimental data do not yet exist. This requires not only robust and reliable CFD methods but also the supporting geometry tools for building the computational models. As a consequence the focus of these studies was not on the cutting edge of CFD technology, but on the more mature technologies that could be relied upon in the heat of battle (i.e. a design project). The primary computational tools used for these studies included a very general three-dimensional panel method, A502/PAN AIR. This method was coupled to a boundary layer analysis code, A598 for viscous analysis. A proprietary geometry system, AGPS, was used to define and construct the computational models. A description of these tools follows.

A502/PAN AIR Panel Method

A502/PAN AIR is a general three-dimensional boundary value problem solver (panel method) for the Prandtl-Glauert equation, references 6 and 7. This equation governs incompressible and linear compressible flows in both the subsonic and supersonic flow regimes. Several important features distinguish A502/PAN AIR from other panel methods. These include: higher order numerics,

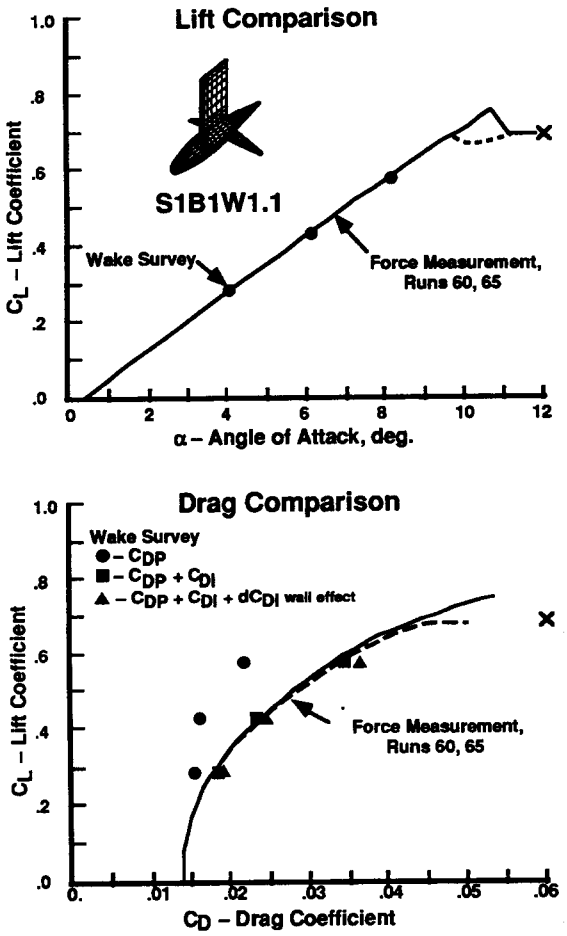

Figure 20. Wake Summary - Force Comparison: S1B1W1.1

These include: higher order numerics, continuity of doublet strength, continuity of geometry, and very general boundary condition options. A502/PAN AIR is a "higher order" panel method, i.e., the singularity strengths are not constant on each panel. In particular, the formulation allows a linear source and quadratic doublet variation on each panel. Continuity of geometry is accomplished by using triangular sub-panels. This approach eliminates gaps in the configuration surfaces, and allows continuous vorticity over the entire configuration. The combination of linear sources, continuous quadratic doublets, continuous surface geometry, and a very robust full direct matrix solver results in a very reliable method for analysis. As a result of these numerical features A502/PAN AIR is very forgiving of irregular paneling, a feature that greatly enhances its practical usability for applications involving complex configurations, such as a hull, keel, rudder and assorted other appendages.

For induced drag calculations a far-field Trefftz plane formulation very similar to that used for the experimental wake analysis is used. The A502/PAN AIR code uses the vortex strengths directly rather than differentiating the lifting surface spanwise loading that can lead to inaccuracies. Reference 8 indicates that the application of the classical Trefftz plane formulation will yield accurate drag values only if there are no drag forces on the wake itself. In the physical world this is automatically taken care of by the wake roll-up. Computationally, it is a much more difficult problem. The routine calculation of wake roll-up from complex geometries to sufficient accuracy for reliable induced drag prediction has not been demonstrated by any method! Fortunately, reference 8, suggests an approach to avoid the problem of drag forces on the wake itself. If the wakes are shed in the freestream direction they may not be force free but they will be drag free. Any drag calculated in the Trefftz plane will then be that of the configuration only, and will not include drag from the wake. This alleviates the need for wake contraction in the computational model and results in a very reliable method for induced drag calculations from complicated geometries. This approach works as long as the configuration lift distribution is not unduly sensitive to the presumed wake trajectory. Lifting surfaces can be modeled as either "thick" (external surface paneling) or "thin" (camberline paneling) surfaces without loss of accuracy in calculating drag.

The A502/PAN AIR code is available through the Advanced Aerodynamics Concepts Branch at the NASA Ames Research Center. Analysis of cases with over 10,000 panels is possible depending on available scratch disk space. Typical cases require between 200 to 3000 panels depending on configuration complexity. Versions of the code have recently been ported to a variety of UNIX based workstations including the IBM R/S 6000.

A598 Viscous Analysis Code

A598, references 9 and 10, is the A502 inviscid panel code coupled with a finite difference boundary layer program. 3-D boundary layer analysis over bodies that lie in the x-z plane of symmetry, and 2-D (with sweep and taper) boundary layer analysis over wing-like surfaces is possible.

The application of the strip boundary layer analysis which includes sweep and taper effects to wing like surfaces is rather straight forward as long as the flow is attached, i.e., no separation. The application of the 3-D boundary layer analysis to bodies is more limited The code is very particular about the types of geometries it will analyze. It works best with bodies that have two planes of symmetry, or can be

analyzed as if they did. This can be applied to canoe hulls and ballast bulbs. For most bodies boundary layer theory will not stay attached for their full length. Such separation prevents calculation of the profile (skin friction + pressure) drag. If the separation is very close to the end of the body, the skin friction calculations are probably valid. The code has been able to calculate attached flow for certain type bodies, including beavertail ballast bulbs.

The A598 code is also available through the Advanced Aerodynamics Concepts Branch at the NASA Ames Research Center.

AGPS - Aero Grid and Paneling System

The key to effective CFD applications is the ability to create computational models in a timely manner. AGPS, Aero Grid and Paneling System, is the key element of this process, references 11 and 12. The use of CFD involves several steps:

- Representation of the vehicle shapes within the computer. This is traditionally called "lofting." This may be done within AGPS or the surfaces may be read in from an external computer aided design (CAD) system. Output surface definitions in the form of IGES files also can be generated for numerical control milling operations of the yacht components.

- Check of the quality of the surfaces. Smoothness of the surface contours is very important from the hydrodynamic standpoint.

- The discritization of the surfaces into a form usable by the particular CFD code. This generates the shape definition to be used by the CFD code. For the A502 program this is called "paneling" and produces the surface network of points such as is shown in Figure 21.

- Analysis of the CFD geometric definition on the supercomputer or the workstation. This produces files containing the detailed surface pressure distributions plus lift and drag data.

- Return of the CFD results to the workstation for review and analysis. This usually involves the plotting of the surface pressure distributions in the form of three-dimensional color contour pictures, and two-dimensional airfoil pressure distribution, spanload, and force plots.

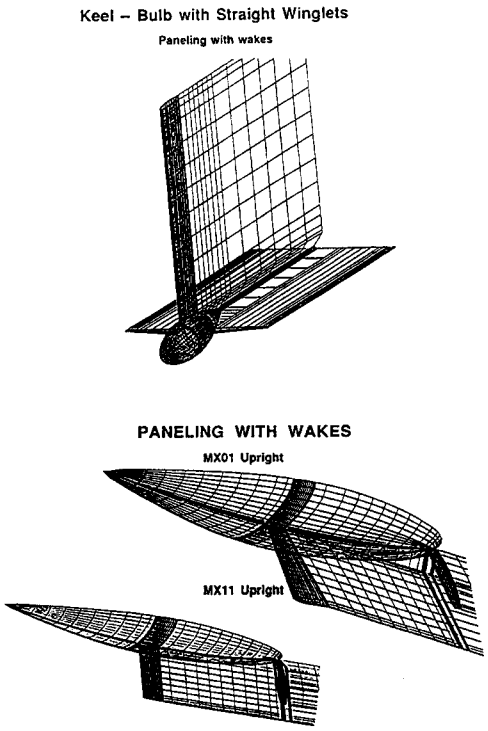

Figure 21. Paneling With Wakes

In the support of the work described in this paper all of the above steps were accomplished by the AGPS program, except for the 2-D plots and, of course, for the CFD solution itself.

AGPS has been in use at Boeing for over ten years. In addition to being a surface lofting system AGPS is a geometry programming language. It is the geometry programming aspects of AGPS that make it such a powerful tool for solving new CFD problems. Because the programming can be done in a unique interactive manner, procedures for generating complex surface lofts, and the subsequent paneling procedures for use in CFD codes can be accomplished in a fraction of the time that it would normally take using a language such as FORTRAN.

Once the paneling procedures have been written the paneling of complete complex configurations is accomplished in a few minutes on the workstation. The result is a file that is ready to submit to the CFD analysis code. These paneling procedures automatically handle all of the surface-surface intersections and the preparation of the surface and wake networks with all of the abutments matching exactly. The paneling procedures developed for the PACT studies included complete yacht configurations consisting of hull, keel, bulb, winglet, rudder, and trailing wake systems. The paneling could be accomplished automatically for both upright and heeled sailing conditions.

COMPUTATIONAL RESULTS

The initial focus of the computational studies was aimed at the use of A502/PANAIR in assessing its applicability to yachting type of geometries, and to evaluating its ability to calculate induced drag. Procedures were developed in AGPS to quickly allow the generation of panel models for input into A502. Paneling models, illustrated in Figure 21, of complete hull-keel-rudder and isolated appendages were supported. Studies to evaluate the accuracy of the Trefftz plane induced drag formulation in A502 were also undertaken. Figure 22 shows a comparison of A502 induced drag results in terms of "e", the span efficiency factor, with classical theory for a bi-plane geometry in which both gap and upper and lower wing span are varied. The wings were modeled as simple rectangular thin surfaces in A502. Excellent agreement with theory is seen for the case where the upper and lower wing span are the same. The agreement deteriorates for wings of unequal span. One source of error is that the spanload distribution in the A502 solution was not constrained to be elliptic as assumed in the theoretical solution. In the Trefftz plane the bi-plane arrangement is very similar to that of a keel and rudder or even a tandem keel. A502 studies were used to determine the optimum rudder and flap settings for minimum induced drag on a hull with keel and rudder at various heel angles. Similar type of calculations have also been carried out for an aircraft configuration and shown to be in good agreement with wind tunnel test data.

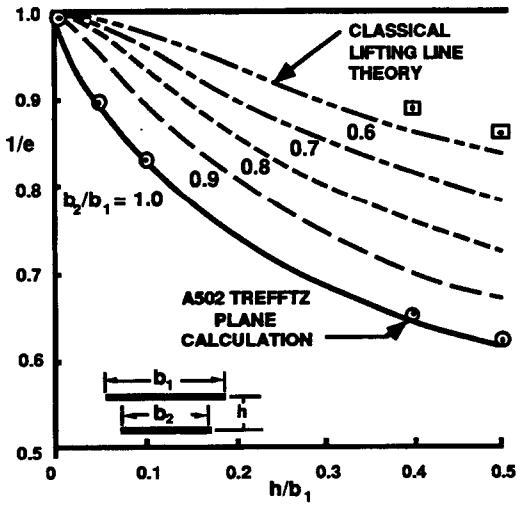

Figure 22. Induced Drag Bi-Plane Gap Study

Another check of the Trefftz plane drag calculation was to compare results with those obtained by integrating pressure over the paneled surface of the

A502 solution with wake in the freestream direction:

Leeway	C_L Integrated	C_D Pressure	C_D Trefftz-plane	Effective Span Ratio
6 degrees	0.243	0.01242	0.01284	0.854
0 degrees	0.0	0.00005	0.0	—

Figure 23. Hull + Keel Induced Drag Test Case

configuration. A comparison of results for a simple hull-keel configuration are shown in Figure 23. Good agreement is seen between the two methods. Integrated pressure calculations require reasonable panel density for accuracy and are not valid for thin surfaces unless the leading edge suction singularity is properly evaluated.

The acquisition of wind tunnel data on the various appendage configurations tested allowed a more through evaluation of the predictive capabilities of A502. Figures 24 to 27 show comparisons of effective draft, keel lift curve slope, and chordwise and spanwise locations of center of pressure. The comparisons are for six configurations that included: keel alone, keel with axisymmetric and beavertail bulb, and both sizes of winglets. Most of the computational results had been generated prior to the wind tunnel test. The agreement with experimental data is excellent in terms of predicting trends and increments between configurations, and very good on predicting performance levels. As is typical of an inviscid method, predicted levels tended to be greater than measured by experiment.

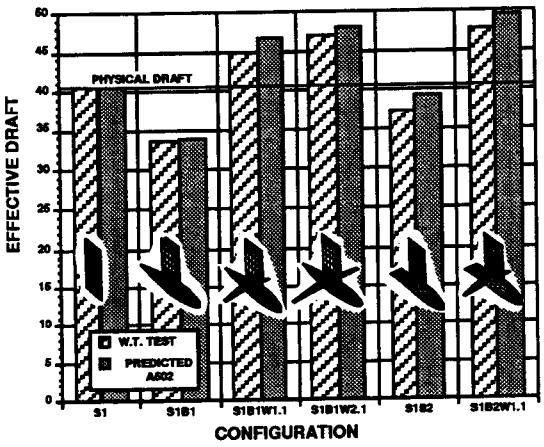

Figure 24. A502 Comparisons with Wind Tunnel Data - - Effective Draft

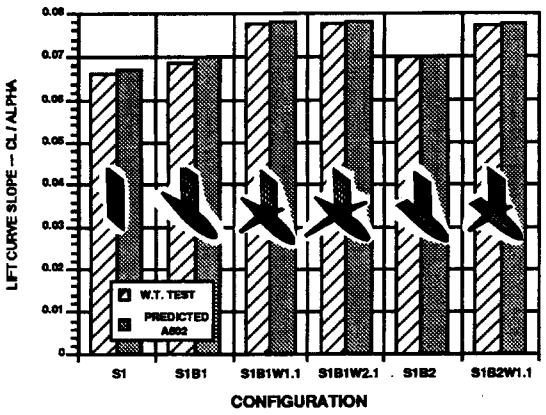

Figure 25. A502 Comparisons with Wind Tunnel Data - Lift Curve Slope

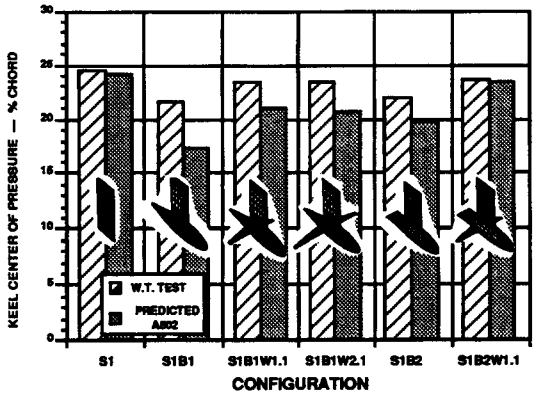

Figure 26. A502 Comparisons with Wind Tunnel Data - Keel Center of Pressure

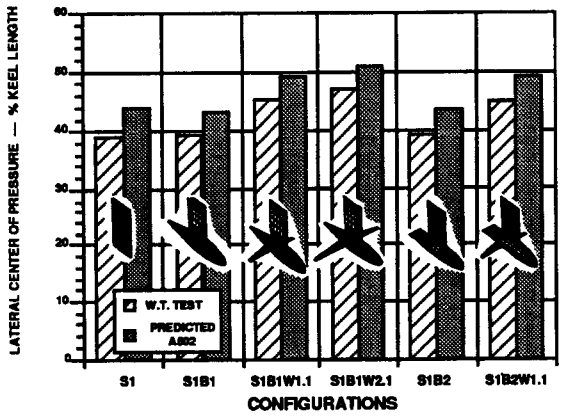

Figure 27. A502 Comparisons with Wind Tunnel Data - Lateral Center of Pressure

Semi-empirical "handbook" methods were used to estimate zero lift drag for the six configurations The comparison with with experimental data are shown in Figure 28. In general, the trends are well predicted, although the estimated drag levels are somewhat higher than the experimental measurements.

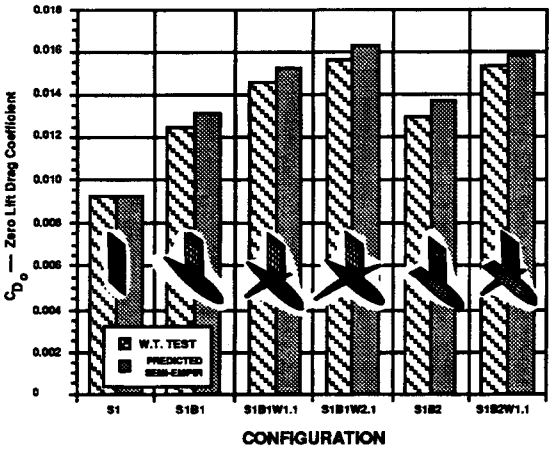

Figure 28. A502 Comparisons with Wind Tunnel Data - Zero Lift Drag

A598 was also used to analyze the viscous characteristics of the wing-like surfaces of the keel and winglets tested at the University of Washington wind tunnel. Attempts to use the code to analyze the viscous characteristics of the two ballast bulbs tested was not successful. "Handbook" estimates were instead made for the two bulbs. Results of these analyses were used to build drag estimates of the configurations. The estimated drags were then compared to force data from the wind tunnel test. The drag build-up consists of the profile drag of the keel and winglets (if present) from the A598 analysis, a "handbook" estimate of the bulb profile drag, and the induced drags calculated by A502. The induced drags and the profile drags from A598 vary as a function of leeway (angle-of-attack). The "handbook" estimate for the bulb is invariant with angle of attack.

A comparison of the total drag build-up with experimental force data for the keel alone is shown in Figure 29. The agreement is very good. Drag build-ups for three other configurations are compared with their respective force data on Figures 30 to 32. For these configurations the agreement is not as good as it was for the keel alone. The build-ups all indicate too high a drag level a zero lift. Shifting the drag build-ups to match at zero lift improves the agreement with the force data. We believe the discrepancy is mainly due to the inaccuracy of the constant "handbook" estimate for the bulb drag.

Improving our ability to predict the installed drag of the large ballast bulbs will continue to be an area of focus. It is unlikely that boundary layer methods will be of significant value in this endeavor. We may have to depend on Navier-Stokes methods to deal with these flows. The information available from the wake surveys should help to develop

and calibrate CFD methods for these applications.

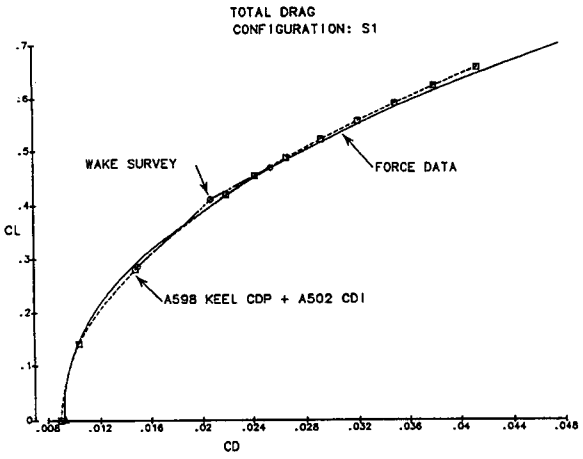

Figure 29. Drag Polar Build-Up: S1

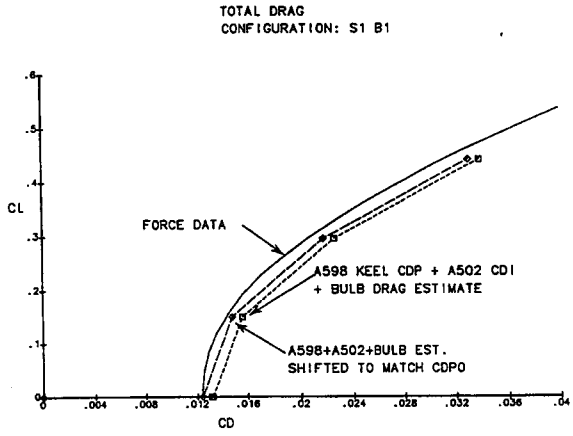

Figure 30. Drag Polar Build-Up: S1B1

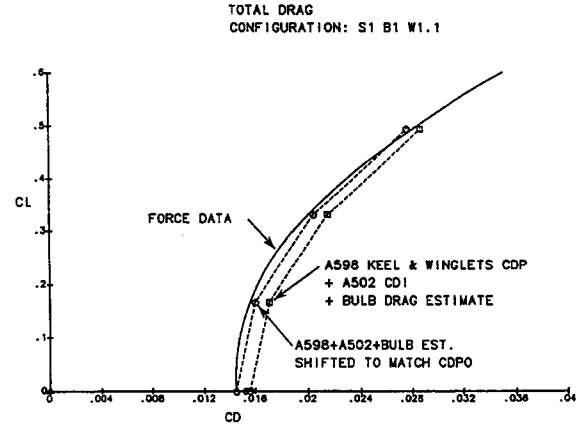

Figure 31. Drag Polar Build-Up: S1B1W1.1

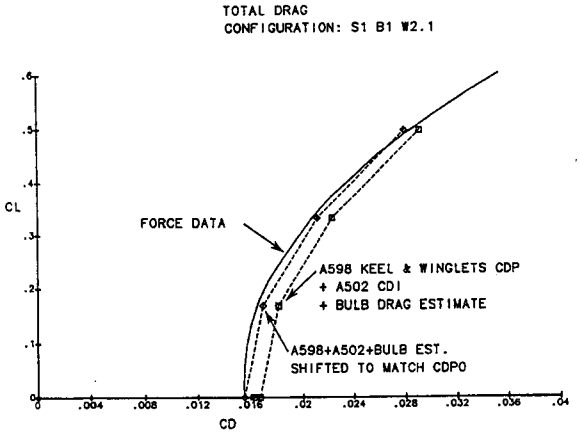

Figure 32. Drag Polar Build-Up: S1B1W2.1

CONCLUDING REMARKS

These studies proved useful in advancing the state of the art in IACC appendage design and analysis. Late in the America's Cup Defender elimination rounds these methods were used to design a new keel and associated appendages for one of the Defense syndicates. On-the-water racing demonstrated a dramatic performance improvement. The existence of the experiment data base and the development of the analysis processes allowed the design work, which involved a series of sequential CFD analyses and geometric refinements, to be accomplished in considerably less than one week!

A502/PAN AIR has proven to be a general and robust panel method that is applicable to the analysis of a variety of aerospace vehicles as well as IACC yachts. The induced drag calculations procedures within the method are well suited for appendage analysis. The boundary layer analysis capability of A598 was applicable for analysis of winglike components such as keel and winglets, but was not always usable on ballast bulb geometries. Reliable viscous analysis methods on three-dimensional bodies such as bulbs and hulls are definitely needed and require further development. AGPS was invaluable in making possible the speedy generation of computational models. This was essential during the very short-fused propriety design work that was undertaken late in the America's Cup campaign.

ACKNOWLEDGMENTS

This work would not have been possible without the support of The Boeing Company in partnership with PACT (Partnership for America's Cup Technology), and the computing resources provided by PACT sponsors; Cray Research, Inc. and IBM. Cray Research provided supercomputer access to the Boeing Computer Services CRAY Y-MP

supercomputer. IBM provided an R/S 6000 workstation to support use of AGPS and some of the CFD computations. Insight gained at the regularly held review meetings with other PACT sponsored researchers was also very beneficial. In addition to the authors listed in this paper, William Herling and Winfried Feifel of The Boeing Company were also involved in related facets of this work not reported in this paper.

REFERENCES

1. Maskell, E. C. "Progress Towards a Method for the Measurement of the Components of the Drag of a Wing of Finite Span," R.A.E. Technical Report 72232, December 14, 1972.

2. Hackett, J. E., Wu, J. C., "Drag Determination and Analysis from Three-Dimensional Wake Measurements," 13th Congress of International Council of the Aeronautical Sciences, Seattle, August 1982.

3. Wu, J. C., Hackett, J. E., and Lilley, D. E., "A Generalized Wake-Integral Approach for Drag Determination in Three-Dimensional Flows," AIAA Paper 79-0279, January 1979.

4. Brune, G. W., "Qualitative Three-Dimensional Low-Speed Wake Surveys," Fifth Symposium on Numerical and Physical Aspects of Aerodynamic Flows, California State University, Long Beach, California, January 1992.

5. Brune, G. W. and Bogataj, P. W., "Induced Drag of a Simple Wing from Wake Measurements," SAE 901934, October 1990.

6. Magnus, A. E. and Epton, M. A., "PAN AIR - A Computer Program for Predicting Subsonic or Supersonic Linear Potential Flows About Arbitrary Configurations Using A Higher Order Panel Method," Vol. 1. Theory Document (Version 1.0), NASA CR-3251, 1980.

7. Saaris, G. R., et al, "A502I User's Manual - PAN AIR Technology Program for Solving Problems of Potential Flow About Arbitrary Configurations," Boeing Document D6-54703, 1989, (also available through NASA Ames Research Center, Advanced Aerodynamics Concepts Branch)

8. Kroo, I., and Smith, S., "The Computation of Induced Drag with Non-Planar and Deformed Wakes," SAE 901933, October 1990.

9. Sullivan, P. P., et. al., "User's Manual for the Viscous Panel Analysis System - Program A598," Boeing Document D6-54744, 1989, (also available through NASA Ames Research Center, Advanced Aerodynamics Concepts Branch)

10. McLean, J. D. and Randall, J. L., "Computer Program to Calculate Three-Dimensional Boundary Layer Flows over Wings with Wall Mass Transfer," NASA CR-3123, 1978.

11. Snepp, D. K. and Pomeroy, R. C., "A Geometry System for Aerodynamic Design," AIAA-87-2902, September 1987.

12. Gentry, A. E., "Requirement for a Geometry Programming Language for CFD Applications," NASA CP-3143, 1992.